J Solid State Electrochem (2017) 21:2021–2027
DOI 10.1007/s10008-017-3589-0

ORIGINAL PAPER

Bio-degradable zinc-ion battery based on a prussian blue analogue cathode and a bio-ionic liquid-based electrolyte

Zhen Liu[1] · **Philipp Bertram**[1] · **Frank Endres**[1]

Received: 16 February 2017 / Revised: 30 March 2017 / Accepted: 31 March 2017 / Published online: 11 April 2017
© Springer-Verlag Berlin Heidelberg 2017

Abstract Rechargeable zinc-ion batteries are of high interest for electrical energy storage due to their low cost, high safety, and good energy density. The development of stable and high-performance cathode materials and environmentally friendly electrolytes is of interest for practical applications. Despite many efforts in pursuing batteries with high energy density and long cycle life, relatively little attention has been paid on the environmental aspects. Thus, bio-batteries that contain nontoxic materials and which are bio-degradable are an interesting alternative to conventional batteries. In the present paper, we present our first results on a highly reversible zinc/prussian blue analogue (PBA) bio-battery, where nanostructured PBA is used as a cathode material, a bio-degradable ionic liquid-water mixture as electrolyte, and zinc as anode. Both the PBA cathode and the zinc anode exhibit good compatibility with the bio-degradable electrolyte. The Zn/PBA battery shows good electrochemical performance including an open circuit voltage of 1.6 V, a specific capacity of ~54 mAh g^{-1} (PBA), and a low self-discharge rate. The zinc anode also shows a good stability since no dendritic growth and shape change are observed after 50 charge-discharge cycles.

Keywords Ionic liquid · Zinc · Prussian blue · Battery · Bio-degradable · Rechargeable

Introduction

Rechargeable batteries are one of the widespread electrical energy storage technologies and have various applications in portable electronic devices, electric vehicles, and grid stabilization [1, 2]. Among a majority of batteries, lithium-ion batteries (LIBs) belong to the most advanced system due to their superior electrochemical performance such as good energy density, high voltage, good cycle life, and low self-discharge [3–6]. However, traditional LIBs, based on the graphite-lithium cobalt oxide interaction chemistry and flammable organic electrolytes, always have safety issue and are expensive.

The development of zinc-based rechargeable batteries, such as zinc-air, zinc-silver, and zinc-bromine batteries, has attracted much attention in recent years due to their low cost, safety, and ease of handling. In the recent decades, considerable efforts have been devoted to alkaline electrolytes, e.g. in zinc-manganese oxide (MnO_2) batteries [7–9]. These batteries have shown good electrochemical performance but have a negative impact on the environment in the case of leakage. In addition, the problems including hydrogen evolution, shape change, and dendritic growth of zinc in aqueous solutions are still major challenges. Recently, zinc-ion batteries with neutral electrolytes [10, 11] and with organic electrolytes [12] have been reported. Nowadays, attention is focused on the exploration of ionic liquid electrolytes [13–15]. The problems associated with hydrogen evolution can be avoided and the dendritic growth of zinc can, in principle, be suppressed in ionic liquids. In addition, ionic liquid-water and ionic liquid-organic solvent mixtures have also been demonstrated to be promising electrolytes for battery applications [16–18]. By the addition of water or organic solvents, the viscosity is lowered and the ionic conductivity is enhanced, which largely improves the performance of the battery. Furthermore, it was also shown

✉ Zhen Liu
zhen.liu@tu-clausthal.de

✉ Frank Endres
frank.endres@tu-clausthal.de

[1] Institute of Electrochemistry, Clausthal University of Technology, Arnold-Sommerfeld-Strasse 6, 38678 Clausthal-Zellerfeld, Germany

that the morphology of zinc deposits obtained by electrodeposition from the ionic liquid 1-ethyl-3-methylimidazolium dicyanamide [emim][dca] containing 3 wt% water was smooth [19]. We previously studied the electrodeposition of zinc from ionic liquids with a water content of 5 to 80 vol% [20] and also found that the structure of the electrolyte transformed from an ionic liquid-like solution to an aqueous-like solution upon the addition of water to more than 40 vol% [21]. Song et al. reported the suppression of zinc dendrites in an aqueous solution with ionic liquids as additive [22]. In comparison with conventional alkaline electrolytes, ionic liquids or ionic liquid molecular solvent mixtures can be regarded as promising electrolytes in battery applications.

Manganese dioxide (MnO_2) has been widely used as cathode material in zinc-ion batteries due to its abundance, low cost, and low toxicity. However, Zn-MnO_2 batteries have some drawbacks such as the formation of by-products, low coulombic efficiency, and poor reversibility during cycling. Therefore, novel cathode materials for zinc-ion batteries were explored, including vanadium oxide bronze ($Zn_{0.25}V_2O_5{\cdot}nH_2O$) [23], NASICON-structured $Na_3V_2(PO_4)_3$ [24, 25], cation-deficient spinel $ZnMn_2O_4$ [26], and prussian blue analogues (PBAs) [27–29]. Among these materials, PBAs are nontoxic, inexpensive, scalable, and easy to synthesize. PBAs as cathode materials in metal-ion batteries have demonstrated long cycle life, high-rate capability, and high coulombic efficiency [30, 31].

In most cases, research attention is focused on new battery technology with high energy density and high power density but hardly on the environmental aspects. Each year, thousands of tons of batteries end up without recycling, containing heavy metals that can harm the environment. Therefore, the development of batteries which are bio-degradable or made from sustainable materials is in our opinion highly desirable. In addition, bio-batteries could have various applications in smartphones, bio-medical devices, and wearable electronics.

Recently, we have shown reversible Zn^{2+} intercalation into PBA nanocubes in bio-ionic liquid-water mixtures [27]. The electrochemical performance is quite good with a flooded half-cell test. In the present work, we have made a “green” battery with zinc powder as anode, bio-degradable ionic liquid choline acetate-water mixtures containing zinc acetate as electrolyte, and PBA as cathode material. The components used in the battery meet the environmental compatibility criteria and safety considerations. Prussian blue is nontoxic as it can be used as an antidote for certain kinds of heavy metal poisoning in medicine. Hexacyanoferrate in PBA does not liberate cyanide compounds until a temperature of 580 °C. The ionic liquid choline acetate is bio-degradable because it is based on vitamin B4. Zinc acetate is a commonly used additive for food supplements. Thus, the battery in combination with all components fully satisfies the desired aspect of environmental compatibility. Most importantly, the first version of this bio-degradable zinc-ion battery exhibits quite a promising electrochemical performance with a cell voltage of ~1.6 V and a capacity of ~54 mAh g^{-1}.

Experimental section

Ionic liquid-based electrolyte The ionic liquid-based electrolyte was prepared by dissolving 1 mol/L zinc acetate ($Zn(OAc)_2$, Sigma-Aldrich, 99%) in the mixtures of choline acetate ([Ch]OAc, IO-LI-TEC, 98%) and water. The amount of [Ch]OAc is 70 wt%. The solution has a viscosity of ~85 mPa s at room temperature, measured by a Bohlin Gemini 150 rheometer (Malvern Instruments, Ltd. UK).

Synthesis of PBA Iron (III) hexacyanoferrate (III) nanoparticles were prepared by a solution precipitation method. First, 500 mL of an aqueous solution of 0.1 mol/L $K_3[Fe(CN)_6]$ was prepared. Then, under continuous stirring, 500 mL of 0.1 mol/L $FeCl_3$ containing 1 mL 32% HCl was added gradually to the above solution. After 30 min, the entire 500-mL $FeCl_3$ solution was added and the suspension gets a brown colour in the beaker. The mixture is then heated to a temperature of 100 °C and maintained for 1 h. The colour of the suspension then changes from brown to dark green. After cooling to ambient temperature, the excess solvent was removed by natural sedimentation. The viscous slurry was washed three times with water to remove residual hydrogen, potassium, and chlorine ions. After washing three times, the suspension has a pH value of 6. The slurry is dried in an oven at a temperature of 100 °C to constant mass, giving a dark green powder.

The following reaction occurs:

$$K_3\left[Fe(CN)_6\right] + FeCl_3 \rightarrow Fe\left[Fe(CN)_6\right]\downarrow + 3KCl$$

Preparation of PBA cathode The PBA cathode was prepared by mixing a slurry of 80 wt% PBA, 10 wt% conductive carbon black (C-Nergy Super C65, Imery, Belgium Ltd.), 2 wt% graphite (Timrex SFG 6, Imery, Switzerland Ltd.), and 8 wt% polyvinylidene fluoride (PVDF, Sigma-Aldrich) in N-methylpyrrolidone (NMP, Sigma-Aldrich). The suspension was stirred overnight at room temperature to a homogeneous paste.

Preparation of the zinc anode The zinc powder gel-like anode was prepared by mixing 80 wt% zinc powder (300 mesh, Grillo zinc oxide, Germany) and 20 wt% electrolyte. The slurry was stirred for 10 min, resulting in a homogeneous paste.

Assembly of the cell The cathode paste is applied, under weight control, directly on carbon cloth (SGL Carbon) with a weight of 95 g m^{-2} and a thickness of 0.15 mm. Then, the cathode was dried at a temperature of 100 °C for 30 min. The calculated mass loading of PBA was ~20 mg cm^{-2}. A glass fiber separator (Hollingsworth & Vose GmbH, Germany), wetted with several drops of the electrolyte, was placed between the cathode and the anode. The button cell (CR2032) was assembled by means of a crimping machine (MTI, type MSK-110) with a pressure of 50 kg cm^{-2}.

Characterization The electrochemical measurement was performed with a VersaStat III (Princeton Applied Research) potentiostat. PBA was used as the working electrode and a zinc anode as counter and reference electrodes, respectively. The structure and morphology of the synthesized PBA were investigated by scanning electron microscopy (SEM, JSM 7610, JEOL) and transmission electron microscopy (TEM, JEM-2100, JEOL). Thermogravimetric measurements (TG) were performed on a TGA 951 analyzer (TA Instruments). The sample was heated from 25 to 500 °C at a heating rate of 10 K/min in a nitrogen atmosphere. The crystal structure was examined by X-ray diffraction (XRD, Empyrean, PANalytical). The content of the metallic elements (K and Fe) was determined by inductively coupled plasma-optical emission spectroscopy (ICP-OES, Vista MPX, Varian), and C, H, O, and N were determined by elemental analysis (Vario EL, Elementar).

Results and discussion

According to the chemical reaction, the formula of the synthesized PBA should be $FeFe(CN)_6$. Elemental analysis (C, H, O N) and ICP-OES results show a K/Fe/CN ratio of 0.01:2.18:6, suggesting that Fe^{3+} was partially reduced to Fe^{2+} during the co-precipitation. The synthesized PBA could be mixtures of $Fe(III)[Fe(III)(CN)_6]$, $Fe(III)_4[Fe(II)(CN)_6]_3$, and $Fe(II)_3[Fe(III)(CN)_6]_2$. We simplified the formula of synthesized PBA as $FeFe(CN)_6$ for short. The TGA curve in Fig. 1a shows a

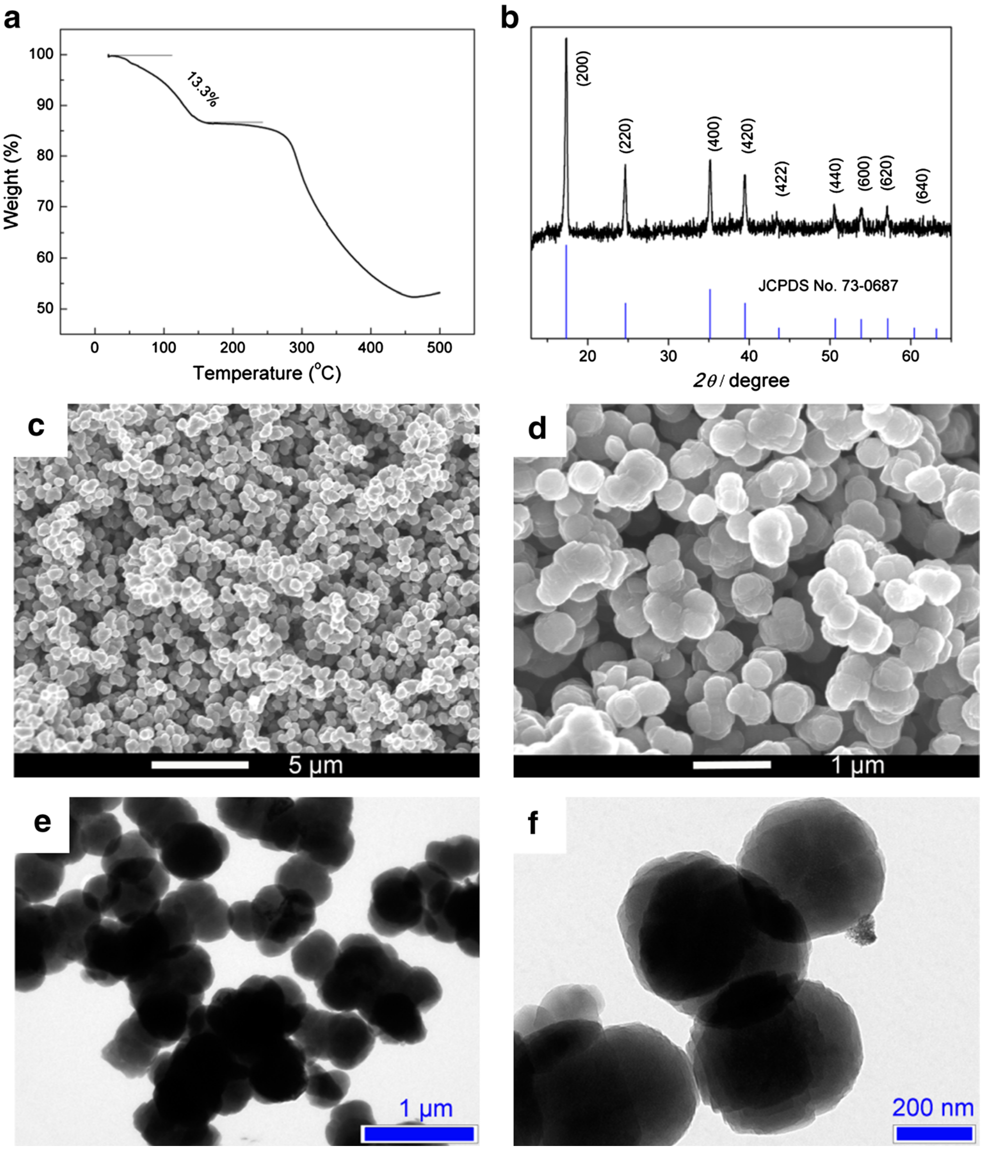

Fig. 1 Characterization of the as-prepared PBA by **a** TGA; **b** XRD; **c**, d SEM; and **e**, **f** TEM

mass loss of 13.3% at temperatures below 150 °C, which corresponds to 2.5 water molecules per mol $FeFe(CN)_6$. Therefore, the formula can be expressed as $Fe[Fe(CN)_6]\cdot 2.5\ H_2O$. The XRD pattern of the PBA is presented in Fig. 1b, showing that the synthesized PBA is crystalline, and all diffraction peaks are consistent with a face-centered cubic structure (JCPDS no. 73-0687). SEM and TEM images of the synthesized $FeFe(CN)_6$ particle show a uniform cubic-shaped structure with an average size of ~300 nm (Fig. 1c–f).

The standard potential of $Fe(III)[Fe(III)(CN)_6]$ is 1.168 V vs. SHE in an aqueous solution [32]. The zinc anode has an electrode potential of −0.76 V under standard conditions. Thus, the maximum theoretical cell voltage is 1.93 V under standard conditions. Our Zn/PBA cell has an average open circuit potential (OCP) of 1.62 V in ionic liquid-water mixtures and can provide sufficient energy to drive a digital clock (Fig. 2a, b). The voltage profile of the cathode during galvanostatic discharging at a current density of 0.1 mA cm^{-2} (0.3 mA, standard discharge current is usually 0.2 mA for a button cell) is shown in Fig. 2c. It seems that the two processes occur during discharging. The first ends at about 1 V, and the second starts. The two Fe(III) ions in $FeFe(CN)_6$ have different electroreactivities. The high-spin Fe(III) coordinated with N atoms of C≡N ligands is more reactive than the low-spin Fe(III) coordinated with C atoms of C≡N ligands. The two steps could be related to the reduction of the two Fe(III), respectively. The initial specific capacity is ~54 mAh $g^{-1}{}_{(PBA)}$ and the specific energy density is 50 Wh $kg^{-1}{}_{(PBA)}$. The galvanostatic discharge and charge voltage profiles of the PBA at a current density of 0.1 mA cm^2 between +1.8 and +0.5 V for 50 cycles are displayed in Fig. 2d. The cut-off charge voltage of the Zn/PBA cell was set at +1.8 V, above which side reactions (e.g. oxygen evolution) could occur, resulting in reduced coulombic efficiencies. The capacity of each cycle is ~50 mAh g^{-1} and there is almost no capacity fading after 50 cycles. A coulombic efficiency of 99.5% is achieved (Fig. 2e), except for the first cycles. During storage, the loss of voltage and capacity of batteries due to self-discharge are inevitable. The synthesized

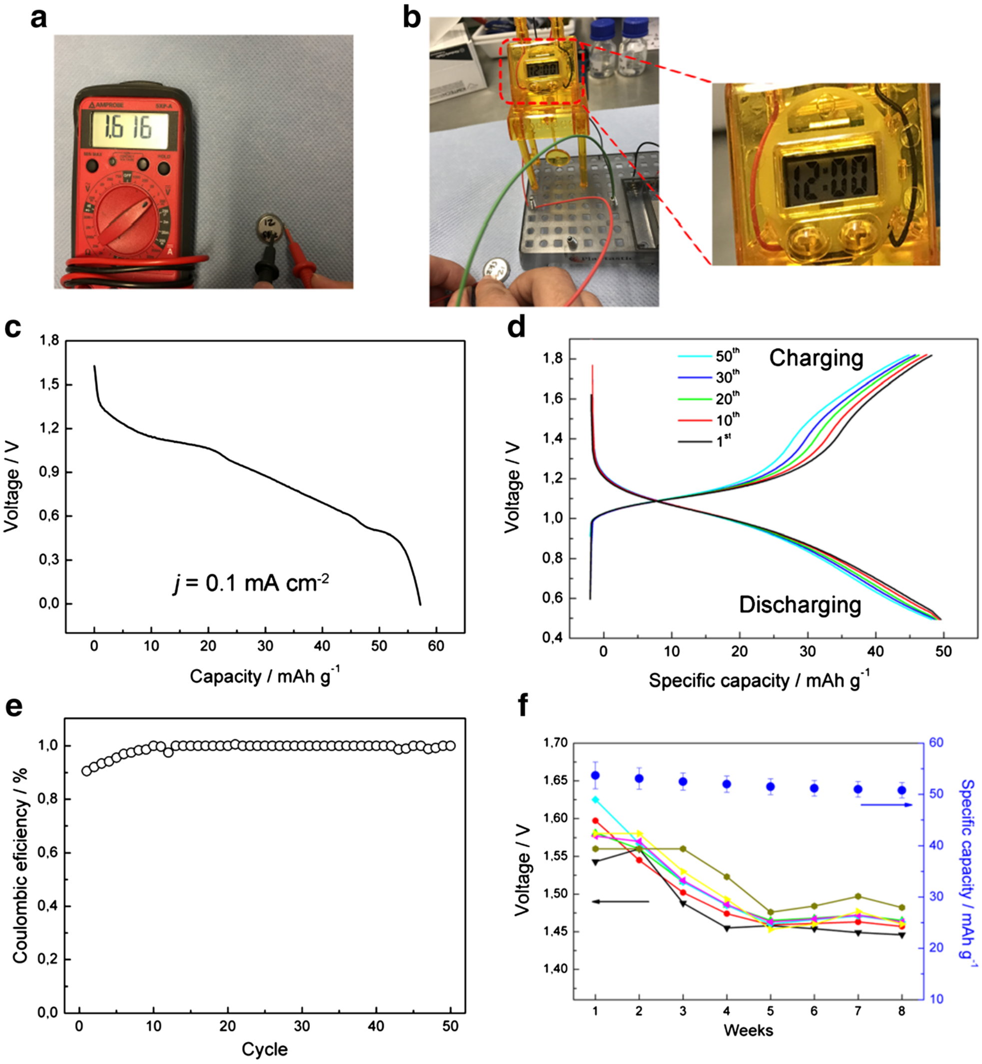

Fig. 2 **a**, **b** Photographs of the freshly prepared Zn/PBA button cell and its application in a digital clock. **c** Voltage profile during discharging at a current density of 0.1 mA cm^{-2}. **d** Galvanostatic charge and discharge curves of the cell between +1.8 and +0.5 V at a current density of 0.1 mA cm^{-2}. **e** Coulombic efficiency of the cell. **f** Self-discharge test by measuring the potential and specific capacity of the cell over 8 weeks

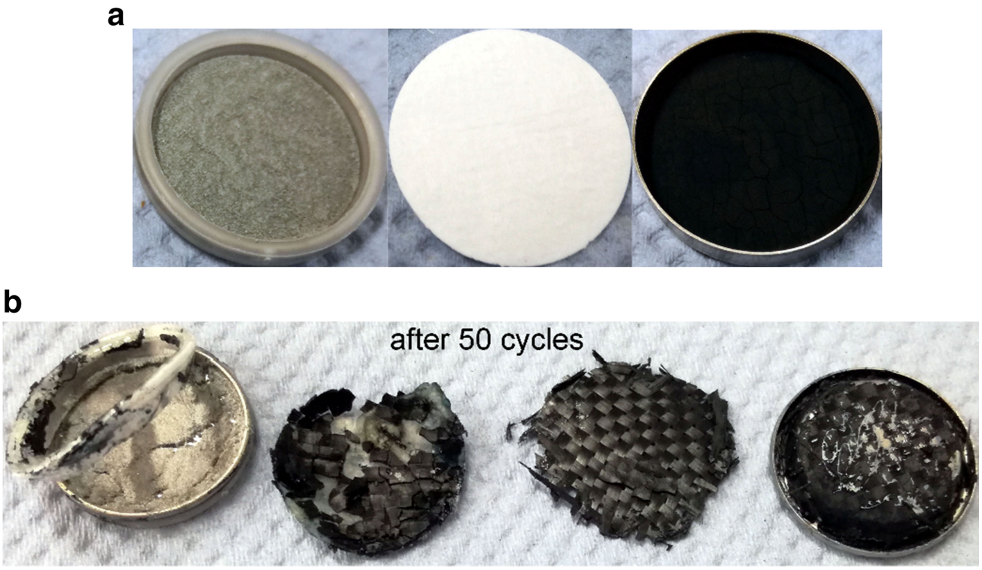

Fig. 3 **a** The Zn/PBA cell with zinc as anode, glass fiber as separator, PBA as cathode, and carbon cloth as current collector before assembly. **b** Disassembled cell after 50 charge and discharge cycles

FeFe(CN)$_6$ in its discharged state could react with the electrolyte or self-decompose, resulting in a drop of the capacity. Therefore, we investigated changes in cell voltage and capacity over a period of 8 weeks at room temperature (Fig. 2f). The OCP of the Zn/PBA cell drops by 0.1 V in 5 weeks and remains quite stable after 6 weeks. The measured capacity fades by 5% in 8 weeks. The results indicate that the PBA might react with the electrolyte at the electrode/electrolyte interface and slightly reduce the voltage and capacity.

The button cell was disassembled after fully discharged at a current density of 0.1 mA cm^{-2} into its components, which visually do not show an obvious damage (Fig. 3). The cathode material is well impregnated with the electrolyte. The dark blue-coloured PBA cathode shows that the electrochemical reduction reaction has taken place as the oxidized Fe(III)[Fe(III)(CN)$_6$] is dark green. The zinc gel-like anode is smooth and has no indication of shape change and dendritic growth. The cathode material was peeled off for analysis and washed with acetone for three times. The SEM image and energy dispersive X-ray (EDX) analysis were shown in Fig. 4. In comparison to the SEM image in Fig. 1c, the particle sizes in Fig. 4 exhibit low volume expansion upon intercalating of the Zn ion. The PB cathode materials have open-framework structure with large channels, which are able to accommodate volume expansion during cycling processes. Therefore, they have demonstrated enhanced electrochemical performance with good life cycle and high-rate capability as cathode materials for battery applications [30, 31]. The EDX analysis shows the presence of the elements fluorine, aluminum, silicon, and chlorine in the cathode material in addition to the previously determined elements in the PBA. The presence of fluorine is due to the use of PVDF as a binder, while the existence of chlorine indicates a residue from the PBA production. The existence of silicon is due to contamination with glass fibers, which takes place during the removal of the cathode material from the separator despite of the greatest care. The presence of aluminum is due to the use of aluminum foil as sample packaging. The most interesting value is the molar ratio of Fe/Zn = 4.4 (an average result of three rectangular areas (~2 × 2 μm) as shown in Fig. 4), allowing the

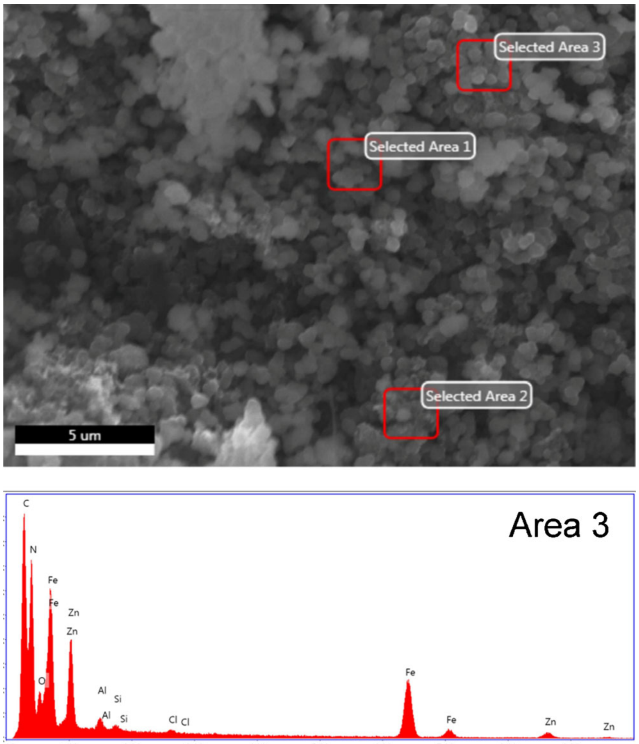

Fig. 4 SEM-EDX of fully discharged PBA cathode at a current density of 0.1 mA cm^{-2}

conclusion that 0.45 mol zinc is intercalated in 1 mol PBA. A molar ratio of Fe/Zn = 2 would be expected if the two Fe(III) are fully reduced. The mechanism of the partial intercalation of zinc in the PBA can result from the following: (i) only the high-spin Fe(III) coordinated with N atoms of C≡N ligands can be electroreduced and (ii) the PBA nanoparticles containing spherical agglomerates inhibit the intercalation of the Zn(II) ions. Therefore, it is conceivable to pursue a new approach in the PBA production, which has more favorable PBA nanostructures for the intercalation.

Conclusion

We have presented the first results on a bio-degradable zinc-ion battery with prussian blue analogue as cathode material, glass fiber as separator, a bio-degradable ionic liquid-water mixture as electrolyte, and zinc as anode. The entire battery fulfills the aspect of environmental compatibility. The Zn/PBA battery has an open circuit voltage of 1.6 V and a specific capacity of 54 mAh g^{-1}. The battery shows stable charge-discharge profiles with a coulombic efficiency of 99.5%. The present battery can afford an energy density of 50 Wh kg^{-1} comparable to lead–acid and Ni–MH batteries. Thus, bio-degradable zinc-ion batteries are potentially interesting in many respects and might be an exciting topic for the future.

Acknowledgements Financial support by the BMBF project LUZI (BMBF: 03SF0499A) is gratefully acknowledged.

References

1. Luo X, Wang J, Dooner M, Clarke J (2015) Overview of current development in electrical energy storage technologies and the application potential in power system operation. Appl Energy 137: 511–536
2. Yang Z, Zhang J, Kintner-Meyer MCW, Lu X, Choi D, Lemmon JP, Liu J (2011) Electrochemical energy storage for green grid. Chem Rev 111:3577–3613
3. Goriparti S, Miele E, De Angelis F, Di Fabrizio E, Proietti Zaccaria R, Capiglia C (2014) Review on recent progress of nanostructured anode materials for Li-ion batteries. J Power Sources 257:421–443
4. Armand M, Tarascon JM (2008) Building better batteries. Nature 451:652–657
5. Goodenough JB, Park K-S (2013) The Li-ion rechargeable battery: a perspective. J Am Chem Soc 135:1167–1176
6. Etacheri V, Marom R, Elazari R, Salitra G, Aurbach D (2011) Challenges in the development of advanced Li-ion batteries: a review. Energy Environ Sci 4:3243–3262
7. Ingale ND, Gallaway JW, Nyce M, Couzis A, Banerjee S (2015) Rechargeability and economic aspects of alkaline zinc–manganese dioxide cells for electrical storage and load leveling. J Power Sources 276:7–18
8. Kordesh K, Weissenbacher M (1994) Rechargeable alkaline manganese dioxide/zinc batteries. J Power Sources 51:61–78
9. Yang C-C, Lin S-J (2002) Improvement of high-rate capability of alkaline Zn–MnO_2 battery. J Power Sources 112:174–183
10. Pan H, Shao Y, Yan P, Cheng Y, Han KS, Nie Z, Wang C, Yang J, Li X, Bhattacharya P, Mueller KT, Liu J (2016) Reversible aqueous zinc/manganese oxide energy storage from conversion reactions. Nat Energy 1:16039
11. Li H, Xu C, Han C, Chen Y, Wei C, Li B, Kang F (2015) Enhancement on cycle performance of Zn anodes by activated carbon modification for neutral rechargeable zinc ion batteries. J Electrochem Soc 162:A1439-A1444
12. Chae MS, Heo JW, Kwak HH, Lee H, Hong S-T (2017) Organic electrolyte-based rechargeable zinc-ion batteries using potassium nickel hexacyanoferrate as a cathode material. J Power Sources 337:204–211
13. Kar M, Simons TJ, Forsyth M, Macfarlane DR (2014) Ionic liquid electrolytes as a platform for rechargeable metal-air batteries: a perspective. Phys Chem Chem Phys 16:18658–18674
14. Macfarlane DR, Forsyth M, Howlett PC, Kar M, Passerini S, Pringle JM, Ohno H, Watanabe M, Yan F, Zheng W, Zhang S, Zhang J (2016) Ionic liquids and their solid-state analogues as materials for energy generation and storage. Nat Rev Mater 1:15005
15. Armand M, Endres F, Macfarlane DR, Ohno H, Scrosati B (2009) Ionic-liquid materials for the electrochemical challenges of the future. Nat Mater 8:621–629
16. Kalhoff J, Eshetu GG, Bresser D, Passerini S (2015) Safer electrolytes for lithium-ion batteries: state of the art and perspectives. ChemSusChem 8:2154–2175
17. Evans T, Olson J, Bhat V, Lee S-H (2014) Effect of organic solvent addition to $PYR_{13}FSI$ + LiFSI electrolytes on aluminum oxidation and rate performance of $Li(Ni_{1/3}Mn_{1/3}Co_{1/3})O_2$ cathodes. J Power Sources 265:132–139
18. Lahiri A, Li G, Olschewski M, Endres F (2016) Influence of polar organic solvents in an ionic liquid containing lithium bis(fluorosulfonyl)amide: effect on the cation–anion interaction, lithium ion battery performance, and solid electrolyte interphase. ACS Appl Mater Interfaces 8:34143–34150
19. Simons TJ, Torriero AAJ, Howlett PC, Macfarlane DR, Forsyth M (2012) High current density, efficient cycling of Zn^{2+} in 1-ethyl-3-methylimidazolium dicyanamide ionic liquid: the effect of Zn^{2+} salt and water concentration. Electrochem Commun 18:119–122
20. Liu Z, Zein El Abedin S, Endres F (2013) Electrodeposition of zinc films from ionic liquids and ionic liquid/water mixtures. Electrochim Acta 89:635–643
21. Liu Z, Zein El Abedin S, Endres F (2015) Raman and FTIR spectroscopic studies of 1-ethyl-3-methylimidazolium Trifluoromethylsulfonate, its mixtures with water and the solvation of zinc ions. ChemPhysChem 16:970–977
22. Song Y, Hu J, Tang J, Gu W, He L, Ji X (2016) Real-time X-ray imaging reveals interfacial growth, suppression, and dissolution of zinc dendrites dependent on anions of ionic liquid additives for rechargeable battery applications. ACS Appl Mater Interfaces 8: 32031–32040
23. Kundu D, Adams BD, Duffort V, Vajargah SH, Nazar LF (2016) A high-capacity and long-life aqueous rechargeable zinc battery using a metal oxide intercalation cathode. Nat Energy 1:16119
24. Zhao HB, Hu CJ, Cheng HW, Fang JH, Xie YP, Fang WY, Doan TNL, Hoang TKA, Xu JQ, Chen P (2016) Novel rechargeable $M_3V_2(PO_4)_3$//zinc (M = Li, Na) hybrid aqueous batteries with excellent cycling performance. Sci Rep 6:25809
25. Li G, Yang Z, Jiang Y, Jin C, Huang W, Ding X, Huang Y (2016) Towards polyvalent ion batteries: a zinc-ion battery based on NASICON structured $Na_3V_2(PO_4)_3$. Nano Energy 25:211–217
26. Zhang N, Cheng F, Liu Y, Zhao Q, Lei K, Chen C, Liu X, Chen J (2016) Cation-deficient spinel $ZnMn_2O_4$ cathode in $Zn(CF_3SO_3)_2$ electrolyte for rechargeable aqueous Zn-ion battery. J Am Chem Soc 138:12894–12901

27. Liu Z, Pulletikurthi G, Endres F (2016) A prussian blue/zinc secondary battery with a bio-ionic liquid–water mixture as electrolyte. ACS Appl Mater Interfaces 8:12158–12164
28. Zhang L, Chen L, Zhou X, Liu Z (2015) Towards high-voltage aqueous metal-ion batteries beyond 1.5 V: the zinc/zinc Hexacyanoferrate system. Adv Energy Mater 5:1400930
29. Trócoli R, La Mantia F (2015) An aqueous zinc-ion battery based on copper hexacyanoferrate. ChemSusChem 8:481–485
30. Wessells CD, Huggins RA, Cui Y (2011) Copper hexacyanoferrate battery electrodes with long cycle life and high power. Nat Commun 2:550
31. Pasta M, Wessells CD, Liu N, Nelson J, Mcdowell MT, Huggins RA, Toney MF, Cui Y (2014) Full open-framework batteries for stationary energy storage. Nat Commun 5:3007
32. Scholz F, Dostal A (1996) The formal potentials of solid metal hexacyanometalates. Angew Chem Int Ed 34:2685–2687